

AD-A076 969

NAVAL RESEARCH LAB WASHINGTON DC
ANOMALOUS TRANSPORT FROM PLASMA WAVES. (U)
OCT 79 W M MANHEIMER
NRL-MR-4066

F/G 20/9

UNCLASSIFIED

SBIE-AD-E000 334

NL

| OF |
AD-
A076969



END
DATE
FILMED

12 79
DDC

AD-E000 334

NRL Memorandum Report 4066

AD A 076969

Anomalous Transport From Plasma Waves

WALLACE M. MANNHEIMER

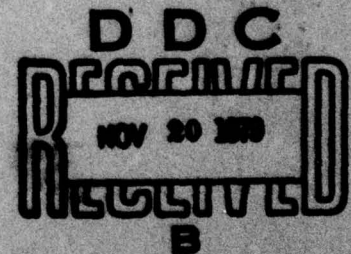
Plasma Physics Division

(12) SC

LEVEL III

October 18, 1979

DDC FILE COPY.



NAVAL RESEARCH LABORATORY
Washington, D.C.

Approved for public release; distribution unlimited.

79 11 07 078

14 NRL-MR-4066

SECURITY CLASSIFICATION OF THIS PAGE (When Data Entered)

REPORT DOCUMENTATION PAGE		READ INSTRUCTIONS BEFORE COMPLETING FORM
1. REPORT NUMBER NRL Memorandum Report 4066	2. GOVT ACCESSION NO.	3. RECIPIENT'S CATALOG NUMBER
4. TYPE (and Subtitle) ANOMALOUS TRANSPORT FROM PLASMA WAVES	5. TYPE OF REPORT & PERIOD COVERED Interim report on a continuing NRL problem	
7. AUTHOR(s) Wallace M. Manheimer	6. PERFORMING ORG. REPORT NUMBER	
8. PERFORMING ORGANIZATION NAME AND ADDRESS Naval Research Laboratory Washington, D.C. 20375	9. CONTRACT OR GRANT NUMBER(s) Memorandum rept.	
11. CONTROLLING OFFICE NAME AND ADDRESS U. S. Department of Energy Washington, D.C. 20545	10. PROGRAM ELEMENT PROJECT, TASK AREA & WORK UNIT NUMBERS NRL Problem No. 67H02-37	
14. MONITORING AGENCY NAME & ADDRESS (if different from Controlling Office) 11 18 Oct 79	12. REPORT DATE October 18, 1979	
	13. NUMBER OF PAGES 33	
	15. SECURITY CLASS. (of this report) Unclassified	
	15a. DECLASSIFICATION/DOWNGRADING SCHEDULE	
16. DISTRIBUTION STATEMENT (of this Report) Approved for public release; distribution unlimited. 18 SBIE 19 AD-E000 334		
17. DISTRIBUTION STATEMENT (of the abstract entered in Block 20, if different from Report)		
18. SUPPLEMENTARY NOTES		
19. KEY WORDS (Continue on reverse side if necessary and identify by block number) Anomalous transport		
20. ABSTRACT (Continue on reverse side if necessary and identify by block number) This is the text of an invited talk on anomalous transport given by the author at the XIVth International Conference on Ionized Gases; Grenoble, France; July 9-13, 1979.		

DD FORM 1 JAN 73 1473

EDITION OF 1 NOV 65 IS OBSOLETE
S/N 0102-014-8601

SECURITY CLASSIFICATION OF THIS PAGE (When Data Entered)

251 950

10B

ANOMALOUS TRANSPORT FROM PLASMA WAVES

Can one derive, from first principles, simple scaling laws for complicated plasma devices like a tokamak? For instance the current vogue is to scale confinement in tokamaks linearly with density; so clearly one would like a thermal conduction coefficient scaling as n^{-1} . The problem is that this thermal conduction must be derived from the quasi-linear and nonlinear theory of very esoteric instabilities. Even if someone could take these instabilities and derive a transport coefficient which had all the right magnitudes and scalings, would anyone else either understand it or believe it?

My own opinion is that one cannot derive simple scaling laws in an understandable, believable way. How then does one explain or predict the behavior of complicated plasma devices which are dominated by anomalous transport? One possibility of course is to use phenomenological transport coefficients, and this may in fact work well. It is certainly likely that current devices could be extrapolated a factor of two in every parameter this way. However this is somewhat unsatisfying, one would somehow like to relate performance to fundamental processes, if only for fundamental scientific reasons. That will be the focus of the remainder of this paper.

Let us look at what is needed to describe a plasma whose transport is dominated by instability. As we will see, there is what might be called a hierarchy of necessary information starting with the simplest questions of stability threshold and proceeding to the most complicated

Manuscript submitted June 29, 1979.

DISTRIBUTION/AVAILABILITY CODES		
Dist.	AVAIL.	and/or SPECIAL
A		

nonlinear theory. How high one has to proceed in this hierarchy is then an indication of how easy and/or how reliable the theory is.

Take for instance a temperature profile in a tokamak plasma, and look at some radius r_0 . The most fundamental question is whether or not the plasma is unstable at this point. If the plasma is stable here, clearly one uses classical transport. If it is unstable anomalous transport should be involved. Thus the first necessary piece of information is the stability threshold. As we will see, there are some circumstances where this is all that is needed to describe the system. Since this description only utilizes the first step in the aforementioned hierarchy, it will surely be the simplest and most reliable theory of anomalous transport. This is the marginal stability theory which we 1-4 and others 5-7 have previously discussed.

The idea behind the marginal stability theory is the following. Imagine a plasma which is stable, but which is forced by some external mechanism to an unstable state. As a concrete example let us consider an ohmically heated tokamak. The current heats the central region and since the edge is cool, an electron temperature gradient is forced upon the system. Let us now postulate that when the electron temperature gradient exceeds some critical value, the plasma becomes unstable. Then at this point, an anomalously large thermal conduction is generated by the instability. A possible functional dependence of K_e on temperature gradient is shown in Fig. 1. This large K_e will cool the plasma, the instability will shut off and K_e will go to its classical value. However once the plasma becomes stable, the ohmic heating will increase its temperature and it will again be driven unstable. Clearly then there is a dynamic balance between heating and anomalous thermal conduction with the plasma sitting at (or perhaps oscillating about) the marginal stability point. The fundamental quantity to determine then is not the turbulent spectrum, but the plasma profile. Once we have the profile, we can calculate the thermal conduction because we know the profile and input power. Once we have K_e , simple quasi-

linear theory gives us the fluctuation level. Thus the logic of a marginal stability calculation is just the reverse of a conventional nonlinear calculation, as shown in Fig. 2.

Now examine the second complication in our hierarchy. Let us say that the marginal stability hypothesis is valid, but there is not one anomalous transport effect but many. To continue with our example of the tokamak, it is known that both electron temperature gradient, and density gradient contribute to instability, and that not only is there anomalous thermal conduction, but also anomalous diffusion. In this case marginal stability does not imply only particular temperature gradient but rather some relation between temperature and density gradient. Then the stability threshold is not sufficient information to determine the profile. One must also know the relation between K_e and D . If one knows the spectrum, and if quasi-linear theory is valid, then one can determine this relation. However now more information is needed than just stability threshold; correspondingly the theory is on somewhat shakier ground than it is if there is only a single anomalous effect.

Let us illustrate how a marginal stability works in a one or two parameter space. First imagine that only temperature gradient drives instability and thermal conduction is the only anomalous process. Then the steady state equations are heat balance

$$0 = \frac{\partial}{\partial x} K \frac{\partial T}{\partial x} + S_i \quad (1)$$

and Marginal stability,

$$\alpha \frac{\partial T}{\partial x} - P = 0 \quad (2)$$

where S_i denote the energy sources. In Eq (2), $\alpha \frac{\partial T}{\partial x}$ is the growth rate which is driven by temperature gradient and P denotes the damping from all sources, for instance shear, ion-ion collisions, etc. The marginal stability approach then consists of using Eq. (2) instead of Eq. (1) as an equation for temperature. Equation (1) is used instead as an equation for K , and it reduces to

W. M. MANHEIMER

$$\frac{d}{dx} K \frac{P}{\alpha} = -S_i. \quad (3)$$

Now imagine that there are two variables instead of one. For instance for the tokamak, say that both density and temperature gradients drive instability and that there is both anomalous diffusion and anomalous thermal conduction. Then the equations which describe the system are heat and particle balance

$$0 = \frac{\partial}{\partial x} K \frac{\partial T}{\partial x} + S_i \quad (4)$$

$$0 = \frac{\partial}{\partial x} D \frac{\partial n}{\partial x} + S_n, \quad (5)$$

marginal stability

$$\alpha \frac{\partial T}{\partial x} + \beta \frac{\partial n}{\partial x} = P \quad (6)$$

and some relation between D and K

$$D = \zeta K, \quad (7)$$

which might come from for instance Quasi-linear theory. Also we assume $\zeta > 0$. These equations can be solved for K as follows. Integrate Eq. (4) from zero to r assuming $\frac{\partial T}{\partial x} = 0$ at $r = 0$ to get

$$K \frac{\partial T}{\partial x} = \int_0^r S_i dx. \quad (8)$$

Then solve for D and $\frac{\partial n}{\partial x}$ from Eqs. (6) and (7), insert in Eq. (5) and integrate from 0 to r.

The result is

$$K = -\frac{\alpha}{P} \int_0^r S_i dx - \frac{\beta}{P \zeta} \int_0^r S_n dx. \quad (9)$$

Then once Eq. (9) is solved for K, we can solve Eq. (4) for T in the standard way.

Let us now examine the conditions under which a solution to Eqs. (4-7) can be formed. In the normal tokamak configuration where the electrons are in the plateau or banana regime,

negative $\frac{\partial n}{\partial x}$ and $\frac{\partial T}{\partial x}$ both drive instability. Therefore α and β have the same sign and both have opposite sign to P . Since, S_T , S_n and ζ are all positive, K is greater than zero so that a solution exists. Now imagine that say the temperature gradient is stabilizing rather than destabilizing, that is α and P now have the same sign. Then, in order to have $K > 0$,

$$\left| \frac{\beta}{P\zeta} \int_0^x S_n dx \right| > \left| \frac{\alpha}{P} \int_0^x S_T dx \right| \quad (10)$$

If inequality (10) is violated in some regions of x , the plasma will be stable and a marginally stable solution does not exist there. In these regions classical transport will apply.

Of course rather than solving equations like (5)-(7), a more practical procedure is usually to use a numerical transport code in which transport coefficients jump to some large value at the stability threshold, and in which the proper relation between the different transport coefficients is also used. As long as these jumps in transport coefficients are handled in a way which is numerically stable, the code will automatically handle the transition not only between stable and unstable plasma, but also between different instabilities.

For the next stage of the hierarchy one must know the nonlinear limit to the fluctuation level. However let us assume that once the fluctuation level is known, the transport coefficients can all be calculated, for instance via quasi-linear theory. Actually this is not as unreasonable as it sounds. Say that the instability is driven by electrons and is stabilized by some nonlinear effect on ions. Then quasi-linear transport coefficients for the electrons should be valid. If this be the case, at least some of the ion transport coefficients can usually be calculated by invoking global conservation relations (for instance energy or momentum conservation, pressure balance, etc). Thus the third level of our hierarchy assumes that transport coefficients can all be calculated in terms of a fluctuation level which is specified by invoking non-linear theory, and/or experiment, and/or numerical simulation of the instability. There are at least

two reasons why the fluctuation level might be required. First, the system may be so strongly driven that nonlinear effects limit the fluctuations to a value smaller than that required to maintain a marginally stable profile. Second, there may be so many anomalous transport effects that there is no simple external mechanism driving the plasma toward instability and no simple relaxation to a stable state because of the instability.

This is the approach recently used at the Naval Research Laboratory to describe anomalous absorption and flux limitation in a laser produced plasma.⁹ Earlier calculations like this also examined hydrodynamic flow in an ionosphere which has been violently perturbed,¹⁰ and the implosion and post implosion phase of theta pinches.^{11,12} Since these results all require a fluctuation level which is the result of a nonlinear calculation they are less reliable than results obtained via calculations on the two lower levels of the hierarchy which we have been describing.

The fourth level of the hierarchy, and the last one which we will describe, is that where both the nonlinear fluctuation level and the transport coefficient are the results of nonlinear calculations. Needless to see results on this level are still more speculative than those on the three lower levels. We will now describe three calculations done at the Naval Research Laboratory which illustrate the three levels. They are calculations of electron and ion temperature profiles in tokamaks⁴, calculation of the structure of transverse resistive shocks³, and calculations of anomalous absorption and thermal energy flux limitation in a laser produced plasma.⁹

In a tokamak, the electron temperature is limited by some anomalous process, generally thought to be instabilities. We have attempted to study this with the use of a simple transport code.⁴ Specifically our code solves the equations

$$\frac{3}{2} n \frac{\partial T_e}{\partial t} = \frac{1}{r} \frac{\partial}{\partial r} R (K_{ce} + K_{an}) \frac{\partial T_e}{\partial r} + E \cdot J - 3v_e \frac{m}{M} n (T_e - T_i) \quad (11)$$

$$\frac{3}{2} n \frac{\partial T_i}{\partial t} = \frac{1}{r} \frac{\partial}{\partial r} r K_{ci} \frac{\partial T_i}{\partial r} + 3 v_e \frac{m}{M} n (T_e - T_i) \quad (12)$$

$$E = J/\sigma \quad (13)$$

where $T_{e(i)}$ are the electron (ion) temperature, J is the current density, E is the toroidal electric field, assumed to be independent of radius, σ is the electrical conductivity.

The current density is assumed to always be at its steady state value, so magnetic diffusion is neglected. Eq. (11)-(13) are solved subject to boundary conditions that $T_e = T_i = 10\text{ev}$ at the limiter, and that the total current is specified. Every term in Eq. (11)-(13) is given by neoclassical theory except for one, the anomalous electron thermal conduction K_{an} . If the plasma is unstable, K_{an} is taken as the Bohm diffusion coefficient K_B . In our study the plasma is subject to one of two instabilities, the internal kink-tearing mode whenever $q = \frac{rB_z}{RB_\theta}$ is less than unity, and the universal drift wave-trapped electron mode whenever the shear strength Θ is below a critical value Θ_{cr} . The value of Θ_{cr} comes from the linear theory of the mode. We will not elaborate here, but a full discussion can be found in Ref. 4. Thus the functional form for K_{an} is

$$K_{an} = K_B \left[\frac{q^{-n}}{1 + q^{-n}} + \frac{(\Theta/\Theta_{cr})^{-n}}{1 + (\Theta/\Theta_{cr})^{-n}} \right] \quad (14)$$

where n^1 and n are large integers, so that K_{an} turns on abruptly as the plasma becomes unstable. Since the quantities in the brackets change abruptly from zero to one, we have called them thermostat functions. Let us now re-emphasize that the nonlinear theory of the instability plays no role in the analysis. The only thing needed to solve Eqs. (11)-(13) is the instability condition which comes only from linear theory.

Now, knowing the profile, one can utilize quasi-linear theory to calculate both the anomalous thermal conduction, fluctuation wave number and fluctuation amplitude. However, even if the behavior is governed by nonlinear theory, the only thing which will be wrong is the calculation of fluctuation level, not the profile.

We will now show some results of the calculation. Since there was not much available data from PLT at the time, we did only one run. The parameters are $B = 35$ KG, $Z_{ef} = 4$, a central density of $n_0 = 4.2 \times 10^{13}$ and a hydrogen plasma. The electron and ion temperature, q , and thermostat functions for q and Θ are given in Fig. 3. Clearly the plasma is in a marginally stable state for internal kink-tearing modes for $0 < \frac{r}{a} < 0.4$, and to trapped electron modes for $0.4 < \frac{r}{a} < 0.9$. The outer region is classical.

Another tokamak which we have simulated is TFR. In TFR more than half of the input power is generally radiated away by impurity radiation¹³. However, as is clearly indicated in Ref. 13, most of this is oxygen line radiation arising from the plasma edge where the temperature is low enough that the plasma is stable. Thus the question is how does the energy get from the center to the edge. Reference 13 also shows that destruction of magnetic surfaces due to internal kink and tearing modes is insufficient to account for this energy transport. Here we examine whether drift and trapped particle instabilities can provide the remainder of the energy transport.

One very interesting experimental result for TFR¹⁵ is that the temperature half width $\Delta r(T)$ depends on only a single parameter, $q(a)$, even though two parameters, B and I are independently varied. Our calculation basically confirms this result. In Fig. 4 is shown (solid line) the predictions by our code for $\Delta r(T)$ as a function of $q^{-1}(a)$.

Here we have assumed $Z_{ef} = 3$ and $n_0 = 6 \times 10^{13}$. Various dots shown the calculated points. Although there is some scatter to the points, $\Delta r(T)$ basically does depend on the single parameter $q(a)$. The dashed line shows the experimental result from TFR.

Another interesting result from the TFR experiment is that the position of the $q = 1$ surface, as defined by the radial position of the node in the saw tooth oscillations in the soft x-ray

signal, also depends only on the single parameter $q(a)$. In Fig. 4 the dash dot line shows that the predicted value for the $q = 1$ surface, as defined by the radial position where the q thermostat function drops to half its maximum value, also depends principally on this single parameter.

In Fig. 5(a) and (b) are predictions of the code for electron temperature compared to experiment, for three discharges having $I = 140$ KA, and $B = 25, 40$ and 50 Kg. Notice that the code does give good agreement with experiment as regards temperature profile. In Fig. 6 are plotted the radial dependence of T_e, T_i, q , for the run with $B = 50$ Kg, $I = 140$ KA.

Other quantities of interest are the $k_{\rho i}$ of the fluctuation and predicted values of $e\phi/T_e$ as a function of radius. These are shown in Fig. 7 for a discharge with 60 KV, 300 KA. The fluctuation level seems to be comparable to that recently reported¹⁴ $e\phi/T_e \approx (3-4) \times 10^{-3}$.

In addition to calculating the temperature profile for TFR, numerous calculations were also done for Alcator. Perhaps the most striking experimental result for Alcator is the increase of energy confinement time with density¹⁵. Our theory does predict this basic dependence. In Fig. 8 is shown the calculated dependence of energy confinement time on central density for three choices of field and current, $B = 50$ KG, $I = 100$ kA; $B = 75$ KG, $I = 100$ kA; and $B = 75$ KG, $I = 150$ kA. In all cases, $Z_{eff} = 1$ and we used a hydrogen plasma. Notice that for central densities less than about $2 \times 10^{14} \text{ cm}^{-3}$, the confinement time increases roughly linearly with density. For larger n_0 the confinement time begins to decrease again.

When the density is sufficiently high however, the plasma is in the Pfirsch Schluter regime, and there is no trapped particle instability. Then the energy confinement time begins to decrease with density. For all three choices of current and field the points with $n_0 = 5 \times 10^{14}$ were completely stable. Not only are there no trapped particle instabilities in the region of

maximum gradient, q was everywhere larger than one so that there are no MHD modes in the center either. Apparently the largest confinement time occurs just on the transition from anomalous to classical thermal conduction. The highest electron temperature however are in the regime of anomalous thermal conduction and low confinement time. In Fig. 9a and b are plotted the radial dependence of T_e and T_i for different densities for the case $B = 75$ kG, $I = 100$ kA. Notice that at low density, where the thermal conduction is anomalous, the temperature profiles are quite peaked. At higher density, where the thermal conduction is classical, the temperature profiles are quite broad.

To summarize, our calculations of tokamak temperature profiles do give qualitative and even some quantitative agreement with measured tokamak temperature profiles. The theory is simple in that nonlinear theory of the instability never enters in. However there are no simple scaling laws which explain tokamak behavior; instead the temperature profiles result only from a numerical solution of the electron and ion energy equations with the appropriate anomalous electron thermal conductivity.

Now we consider a different plasma configuration, a cross field collisionless resistive shock. Here, as we will see, marginal stability appears to be a viable concept, but two transport processes, electron and ion heating play important roles. In a shock, fluid convection (that is the $V \frac{dv}{dx}$ term in the momentum equation) tends to steepen the density profile. Since the magnetic field is frozen into the flow it also steepens and the current thereby increases. However at some point, the current becomes so great that ion acoustic waves are driven unstable. These waves then grow, the anomalous resistivity increases, and the shock profile will then tend to broaden. The shock profile will then be determined by the condition that ion acoustic waves are everywhere marginally stable, that is³

$$\frac{c}{4\pi ne} \frac{dB}{dx} = \left(\frac{T_e}{2M} \right)^{1/2} \left[1 + \left(1 + 12 \frac{T_e}{T_e} \right)^{1/2} \right]$$

$$\times \left\{ 1 + \frac{M}{m} \left(\frac{T_e}{T_i} \right)^{3/2} \exp \left\{ -\frac{4T_e}{T_i} \left[1 + \left(1 + 12 \frac{T_e}{T_i} \right)^{1/2} \right] \right\} \right\} \quad (15)$$

From the Rankine-Hugoniot relations, the magnetic field, density and temperature are known are all known upstream and downstream. Thus, once we know $\frac{T_i}{T_e}$, the ion to electron temperature ratio, we can estimate $\frac{dB}{dx} \approx [B(\text{upstream}) - B(\text{downstream})]/L_s$, and thereby estimate the shock width L_s .

The problem now is to estimate the ion to electron temperature ratio. For an ion acoustic wave at marginal stability, this can be done by comparing the heating rates of ions and electrons. Say that the ion wave transfers momentum from ions to electrons at a rate P . Then it can be shown, from resonant quasi-linear theory, that in the reference frame in which the ions are at rest, energy is transferred from electrons to ions at a rate $(\omega/k)P$, where (ω/k) is the phase velocity of the ion acoustic wave. If the electron drift velocity is denoted u , then momentum and energy conservation equations for electrons and ions read

$$nm\bar{u} = -P \quad (a) \quad (16)$$

$$nm\bar{u}u + 3/2 n T_e = -\frac{\omega}{k} P = -\frac{3}{2} n T_i \quad (b)$$

From Eqs. (16a and b), it is a simple matter to solve for the ratio of heating rates,

$$\frac{T_e}{T_i} = \frac{(u - \omega/k)}{(\omega/k)} \quad (17)$$

If both electrons and ions are substantially heated by the shock, the temperature ratio should be roughly equal to the ratio of heating rates, or

$$\frac{u - \omega/k}{\omega/k} \approx \frac{1}{\sqrt{2}} \left[1 + \left(1 + 12 \frac{T_e}{T_i} \right)^{1/2} \right]^{1/2} \left[1 + \frac{M}{m} \left(\frac{T_e}{T_i} \right)^{3/2} \exp \left\{ -\frac{T_e}{T_i} \left[1 + \left(1 + 12 \frac{T_i}{T_e} \right)^{1/2} \right] \right\} \right] - 1 \approx \frac{T_e}{T_i} \quad (18)$$

Equation (18) is a transcendental equation for $\frac{T_e}{T_i}$. For a hydrogen plasma, we find $\frac{T_e}{T_i} \sim 7.5$.

Then knowing $\frac{T_i}{T_e}$, Eq. (15) gives a simple estimate for shock width. For

$$\frac{\omega_{pe}}{\omega_{ce}} \approx 70, \quad \frac{c}{4\pi n e} \frac{\Delta B}{L_s} \approx 7.5 \sqrt{\frac{T_e}{M}} \frac{4\pi n T}{B^2} \approx 0.01, \quad (19)$$

and a Mach two shock, this gives the result $L_s \sim 10c/\omega_{pe}$ which is consistent with the transverse shock experiments done at Culham laboratory.¹⁶ From this estimate of shock width, one can calculate a resistivity and from the resistivity, a fluctuation level. This works out to be about

$$\left(\frac{e\phi}{T_e} \right)^2 \sim 5 \times 10^{-3}. \quad (20)$$

Let us re-emphasize that at no point in This calculation was an estimate of $\frac{e\phi}{T_e}$ from nonlinear theory ever required.

Actually, one can do much better than estimate these quantities. In Ref. 3, fluid equations for n , T_e , T_i and B , coupled to wave equations for 16 (or 64) ion acoustic fluctuations (at different wave vector) are numerically integrated from upstream to downstream. The waves are assumed to grow or damp at the local linear growth or damping rate, and quasi-linear theory is used to calculate resistivity as well as electron and ion heating rate. It was found that the shock profile did in fact remain at a marginally stable current for nearly the entire shock profile. Results of such a calculation are shown in Fig. 10 where spatial profiles of n , B , T_e , T_i and $\left(\frac{e\phi}{T_e} \right)^2$ are shown. To summarize, the structure of transverse resistive shocks in hydrogen seems to be consistent with ion acoustic waves being at marginal stability everywhere in the profile. Estimates and calculations of shock width and fluctuation level are in good quantitative agreement with experiments.

As a final example, we consider the absorption of laser light in a laser produced plasma. This is discussed much more fully in Ref. 9 and the description here will be very brief. The idea is to use a numerical solution of the fluid and wave equations with anomalous transport. There are two instabilities which provide this anomalous transport. First, there is Brillouin

backscatter, where in the laser light decays into a reflected wave and an ion acoustic wave; and second, there is an ion acoustic instability generated by the return current.

For Brillouin backscatter, if the growth rate in homogeneous media is γ_0 , then the spatial amplification in inhomogeneous for either an undamped,¹⁷ or strongly damped¹⁸ ion acoustic wave, is

$$\exp \frac{2\pi\gamma_0^2 L_{ph}^2}{\sqrt{\frac{T_e}{M}c}}$$

where L_{ph} is the size of the region of phase coherence between incident, reflected, and ion acoustic wave. This amplification turns out to be so large that any theory based upon it will give nearly total backscatter in virtually any circumstance. However when examining the amplitude of the ion acoustic wave generated, one sees that it is very large, so large that any ion trapping should be very important and linear theory of the instability invalid. Thus a description of the process has to be based on a nonlinear description of the instability. Earlier theory^{19, 20} has shown that if trapping is important one way the instability can be modeled is by reducing the growth rate γ_0 by a factor of between about five and ten. We have adopted such an approach to model the effect of Brillouin backscatter. Thus we need not only a nonlinear theory of the fluctuation amplitude, but also a nonlinear reduction in the reflection due to stimulated Brillouin backscatter.

The second instability which we consider is the ion acoustic instability driven by a return current. If electrons conduct heat but carry no current, a flux of energetic particles in one direction is balanced by a flux of low velocity particles going the other way. This return current can drive ion acoustic waves unstable. There are three principle effects of this instability; first the electron thermal conductivity is reduced; second, there is an electron ion energy exchange; and third, there is anomalous absorption of laser light resulting from the scattering of laser light

on the ion density fluctuations. A linear and quasi-linear theory of this instability has been published recently,²¹ and a self consistent steady state treatment of the coupling of anomalous absorption and flux limitation has also been presented.²² Here, a fluctuation level is required, but then with this fluctuation level, the transport coefficients are related by Quasi-linear theory.

The approach in Ref. 9 is to numerically solve the fluid equations where anomalous transport and backscatter results from these two instabilities. We have simulated three types of Nd laser pulses. First single short (70p sec) pulses on a target which has an initial density gradient scale length of 10μ . This simulates many of the short pulse experiments, especially on slab targets. We find that the absorption is principally resonant absorption, but it gets a strong boost from return current driven turbulence. From irradiances of 10^{14} W/cm² to 3×10^{16} W/cm² the absorption is about 40%, with about 25% resonant absorption (also shown in Fig. 11, is backscatter and specular reflection vs. irradiance.) This is in reasonable agreement with data taken from many laboratories. In Fig. 12 are shown expansion velocity, electron temperature and flux limit, Q/nmV_e^3 , as a function of irradiance. The points are measured electron temperatures from the NRL experiment.²³

A second simulation is of a double structured pulse. Recent experiments at NRL have shown that if the main laser pulse illuminates a prepulse formed plasma, very strong backscatter results.²⁴ We model this by assuming a 100μ m scale length for $n < 0.1n_{cr}$ and a 30μ scale length for $N > N_{cr}$ and illuminate with a single 70p sec pulse. Shown in Fig. 13 is absorption, backscatter, resonant absorption and specular reflection as a function of irradiance. Also shown are experimental measurements of backscatter as a function of irradiance. Clearly there is good qualitative agreement between theory and experiment here.

Finally we have simulated long pulse experiments also. Here we assume a gradient scale length of 100μ and take a pulse which rises up to a final steady irradiance and then remains

constant. In Figs. 14 and 15 are shown plots of absorption, backscatter and specular reflection versus irradiance; and then plots of electron temperature, expansion velocity and flux limit versus irradiance. The points on the figures are experimental measures of absorption^{25, 26} for long pulse experiments. To summarize, the fluid simulation with anomalous transport seems to provide qualitative and even fair quantitative agreement with experiments on laser produced plasmas for a variety of laser pulse shapes and over nearly five orders of magnitude in irradiance.

Now what about our initial question concerning whether simple scaling laws can be derived from first principles? The entire thrust of this paper is that they really cannot. However this does not mean that no progress can be made; on the contrary it seems that one can go far with fluid simulations with the instability entering via anomalous transport. In some cases, all that is needed for good modeling is the linear stability threshold. In other cases nonlinear theory and/or relation between different transport coefficients is needed. However in all cases, the scaling comes from a numerical solution of the fluid equations, not from a simple scaling law.

REFERENCES

1. W.M. Manheimer and J.P. Boris, Comments on Plasma Physics, **3**, 15 (1977).
2. W.M. Manheimer, K.R. Chu, E. Ott and J.P. Boris, Phys. Rev. Lett., **37**, 286 (1976).
3. W.M. Manheimer and J.P. Boris, Phys. Rev. Lett., **28**, 659 (1972).
4. W.M. Manheimer and T.M. Antonsen, Phys. Fluids, May, 1979.
5. C.F. Kennel and H.E. Petchek, J. Geophysical Res. **71**, 1 (1966).
6. J.P. Christiansen and K.V. Roberts, Nucl. Fusion, **18**, 181 (1978).

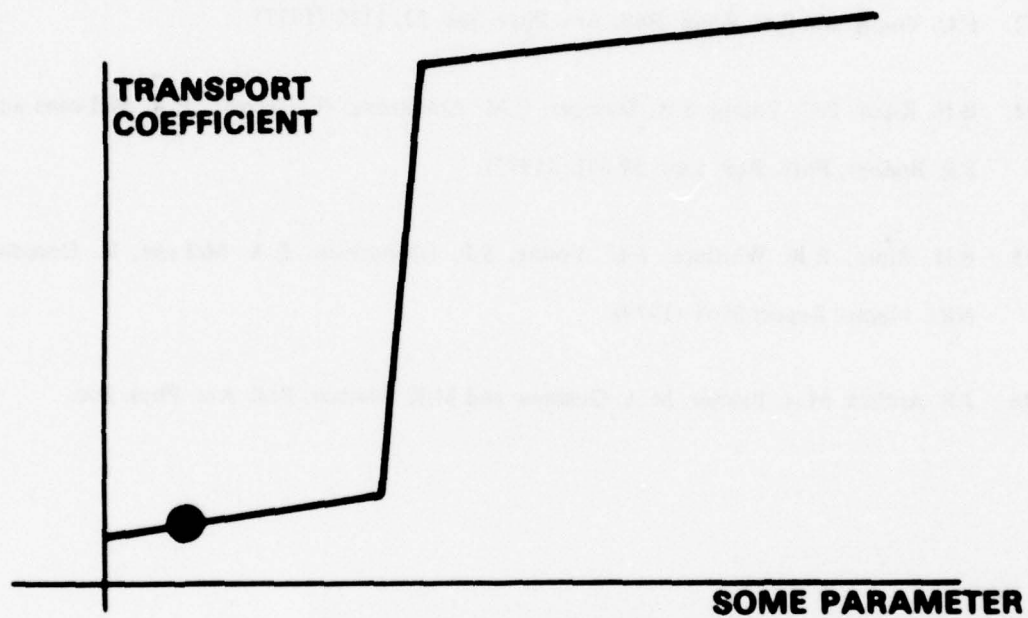
W. M. MANHEIMER

7. H.L. Berk and J.J. Stewart, Phys. Fluids **20**, 1080 (1977).
8. W.M. Manheimer, *An Introduction to Trapped Particle Instability in Tokomaks*, Chapter II ERDA Critical Review Series.
9. D.G. Colombant and W.M. Manheimer, Phys. Fluids to be published.
10. M. Lampe, W.M. Manheimer and K. Papadopoulos, NRL Memo. Report 3076, June 1975.
11. B. Hui, R.C. Davidson and S. Hamasaki, Nucl. Fusion, **16**, 73 (1976).
12. S. Hamasaki and N.A. Krall, Phys. Fluids **20**, 229 (1977).
13. Equipe TFR, IAEA Conference, Berchtesgaden, W. Germany, October 1976, paper IAEA CN-35/A3.
14. TFR Group (presented by F. Koechlin) 8th European Conference on Controlled Fusion and Plasma Physics, Prague, Sept. 1977.
15. E. Apgar, B. Coppi, A. Gondhalekar, H. Helava, D. Komm, F. Martin, B. Montgomery, D. Pappas, R. Parker and D. Overskei, IAEA Conference, Berchtesgaden, W. Germany, Oct. 1976, Paaper IAEA 35/A6.
16. J.W.M. Paul, C.C. Daughney and L.S. Holmes, Phys. Rev. Lett. **25**, 497 (1970).
17. M.N. Rosenbluth, Phys. Rev. Lett., **29** 565 1972.
18. Nishakawa in Advances in Plasma Physics, Volume 6, A. Simon and W. Thompson, editors.

NRL MEMORANDUM REPORT 4066

19. W.M. Manheimer and R. Flynn, Phys. Fluids 17, 409 (1974).
20. W.M. Manheimer and H.H. Klein, Phys. Fluids 17, 1889 (1974).
21. W.M. Manheimer, Phys. Fluids 20, 265 (1977).
22. W.M. Manheimer, D.G. Colombant and B.H. Ripin, Phys. Rev. Lett 28, 1135 (1977).
23. F.C. Young and B.H. Ripin, Bull. Am. Phys. Soc. 22, 1112 (1977).
24. B.H. Ripin, F.C. Young, J.A. Stamper, C.M. Armstrong, R. Decoste, E.A. McLeans and S.E. Bodner, Phys. Rev. Lett. 39 611, (1977).
25. B.H. Ripin, R.R. Whitlock, F.C. Young, S.P. Obenschain, E.A. McLean, R. Decoste, NRL Memo. Report 3965 (1979).
26. J.P. Anthes, M.A. Palmer, M.A. Gusinow and M.K. Matzen, Bull. Am. Phys. Soc.

INTERFACE WITH FLUID CODES



FOR A WIDE RANGE OF EXTERNAL SOURCE STRENGTHS, FLUID CODE WILL AUTOMATICALLY PICK OUT A marginally stable profile.

Fig. 1 — A possible plot of transport coefficient versus some relevant parameter.

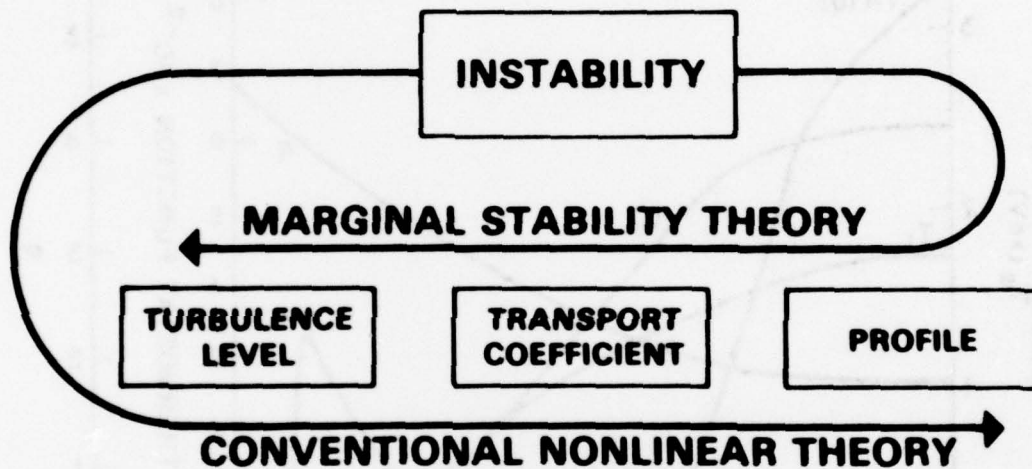


Fig. 2 — Logic of a marginal stability calculation contrasted to the logic of a conventional nonlinear calculation.

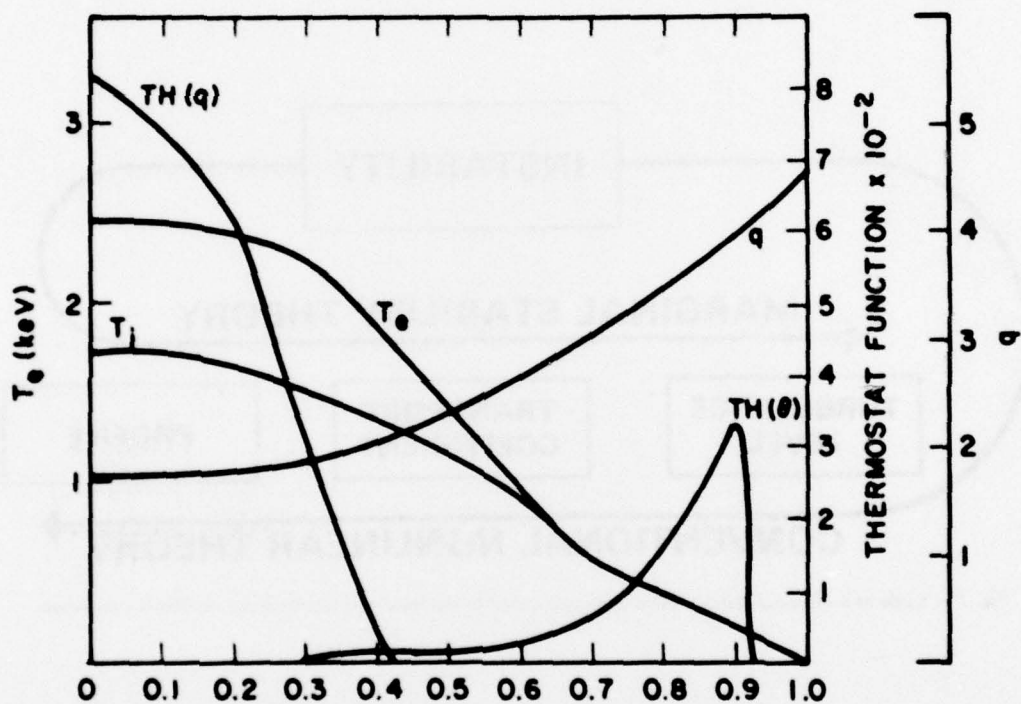


Fig. 3 — PLT electron and ion temperature profiles showing regions of fluid and micro instability.

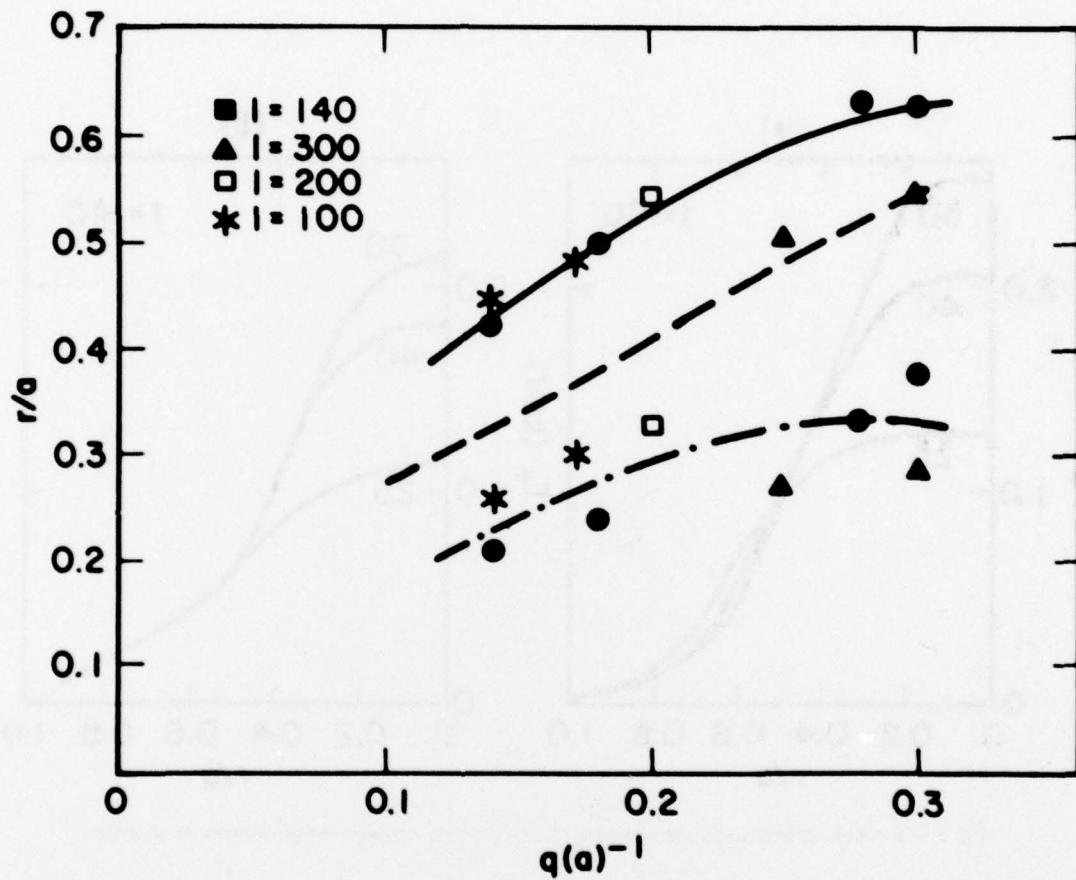


Fig. 4 — Temperature half-width and width of the $q(r) = 1$ region in TFR as a function of $q(a)^{-1}$. The solid and dash-dot line are approximate fits to the numerically obtained data points. The dashed line is the experimentally observed temperature half-width.

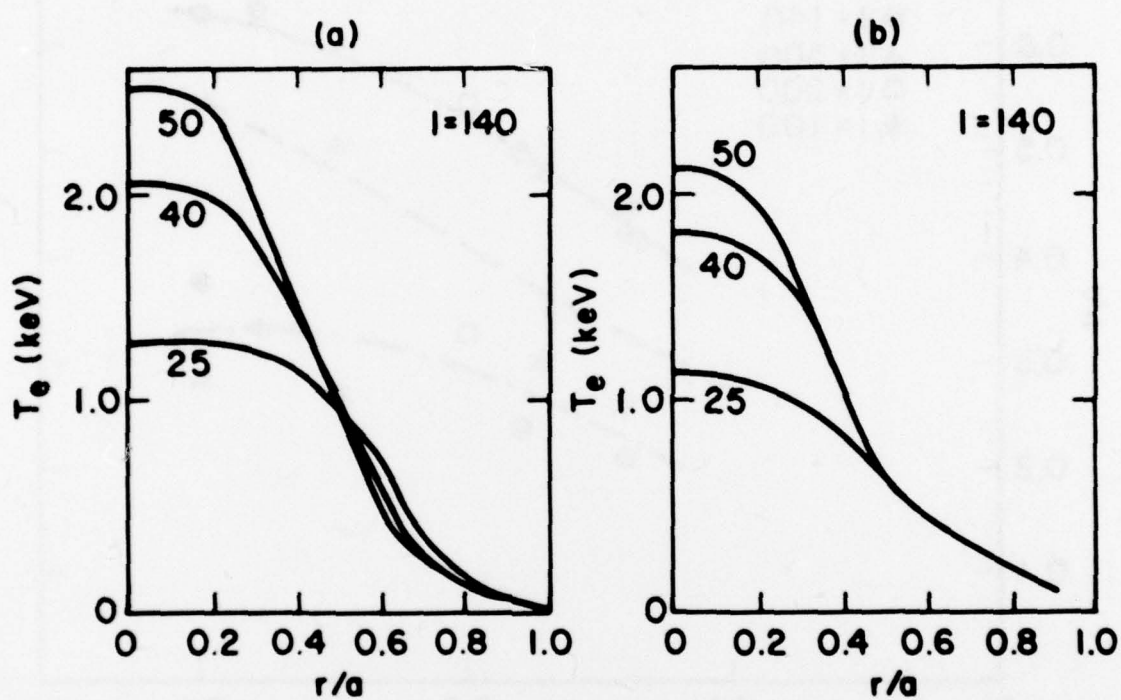


Fig. 5 - Electron temperature profiles in TFR. (a) numerically obtained (b) experimentally obtained.

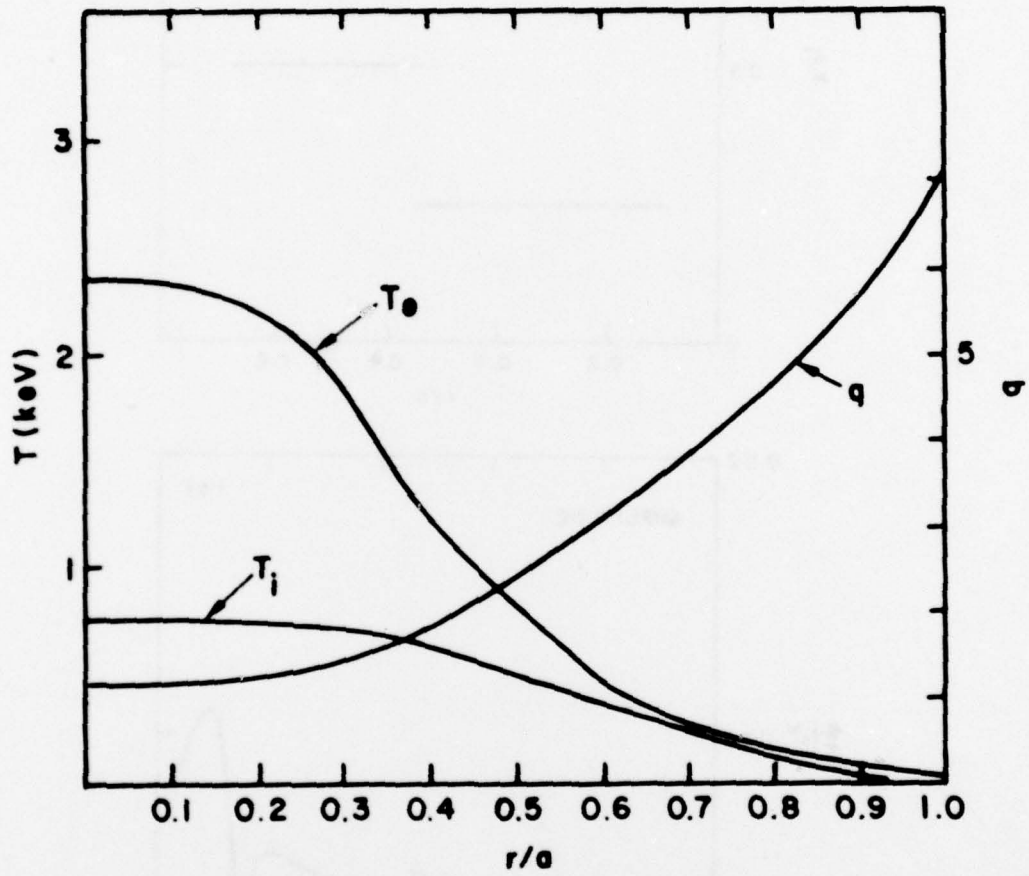


Fig. 6 - TFR electron and ion temperature profiles.

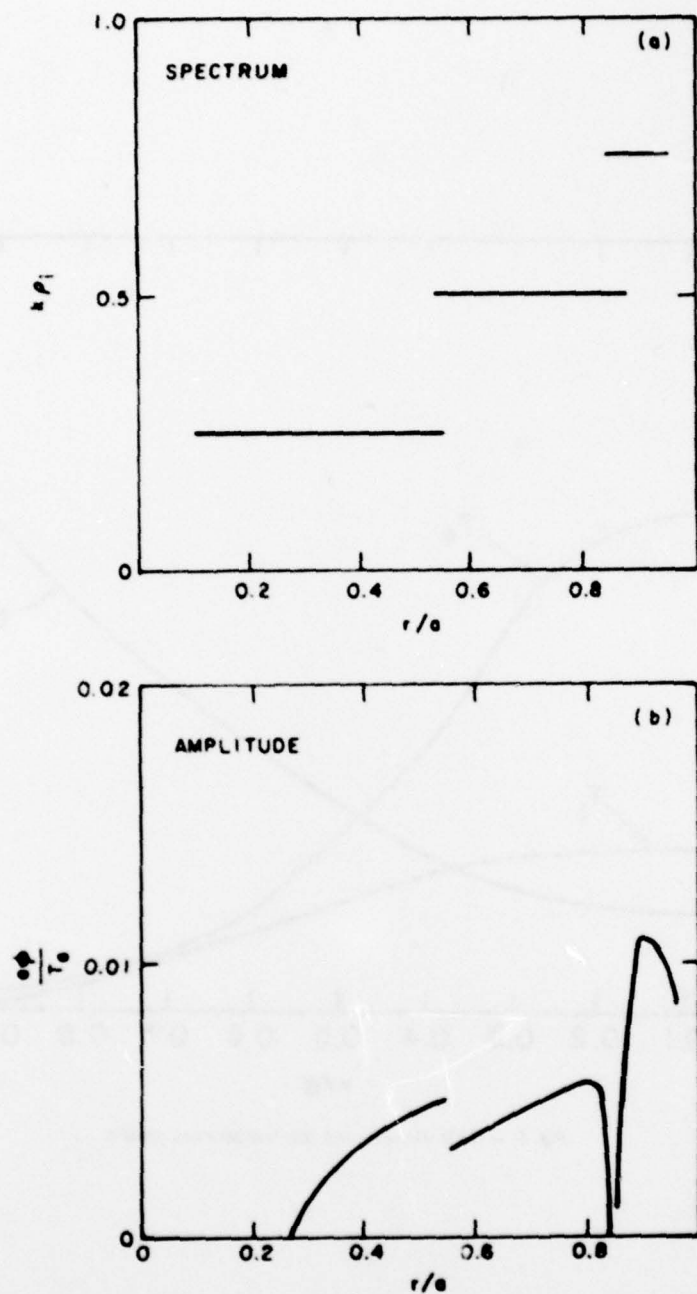


Fig. 7 — (a) The most unstable mode in TFR as a function of r/a , and (b) the fluctuation level implied by the numerically determined anomalous transport.

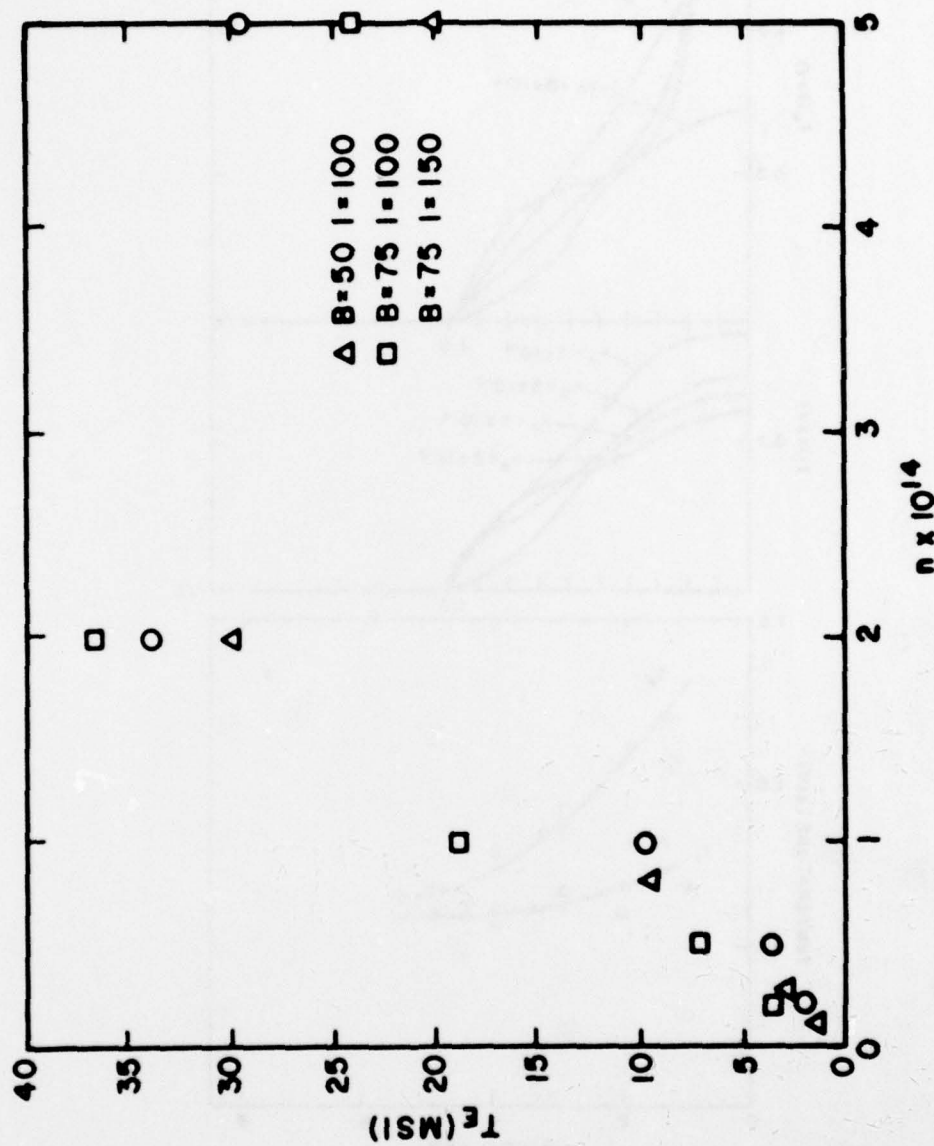


Fig 8 - Energy confinement time versus central density in Alkator.

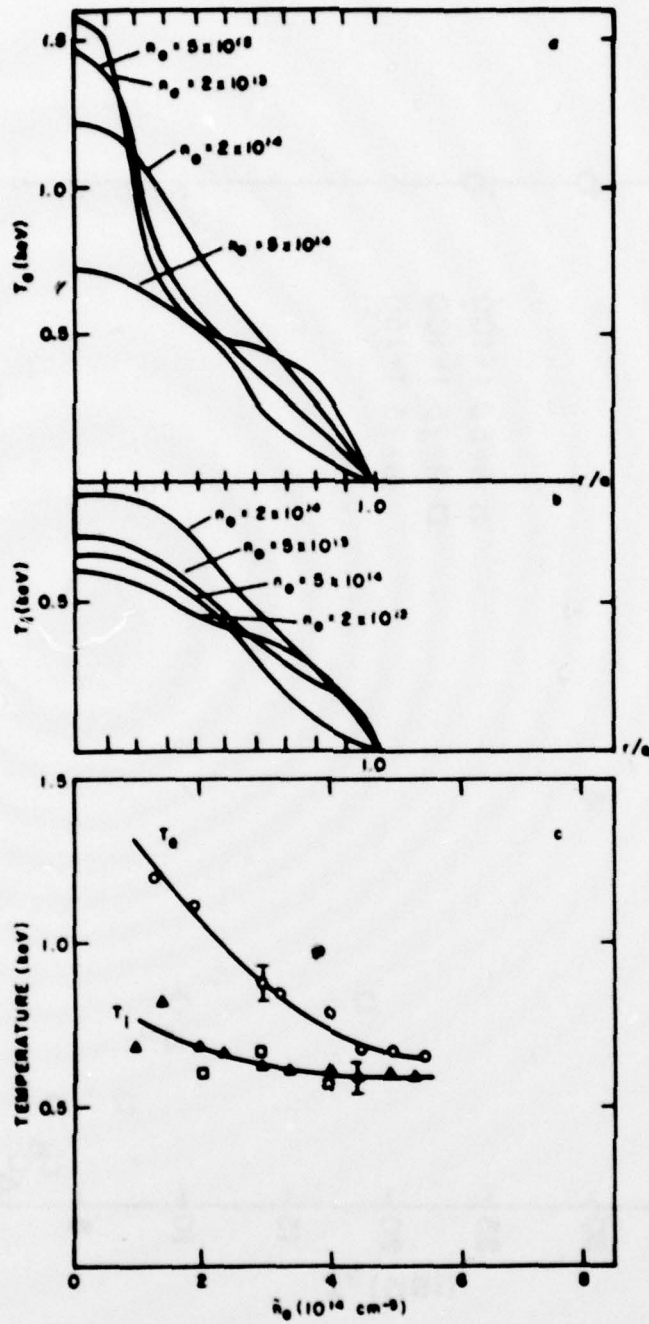


Fig. 9 — Calculated electron (a) and ion (b) temperature profiles at different densities. Also, a plot (c) of measured central electron and ion temperatures vs density.

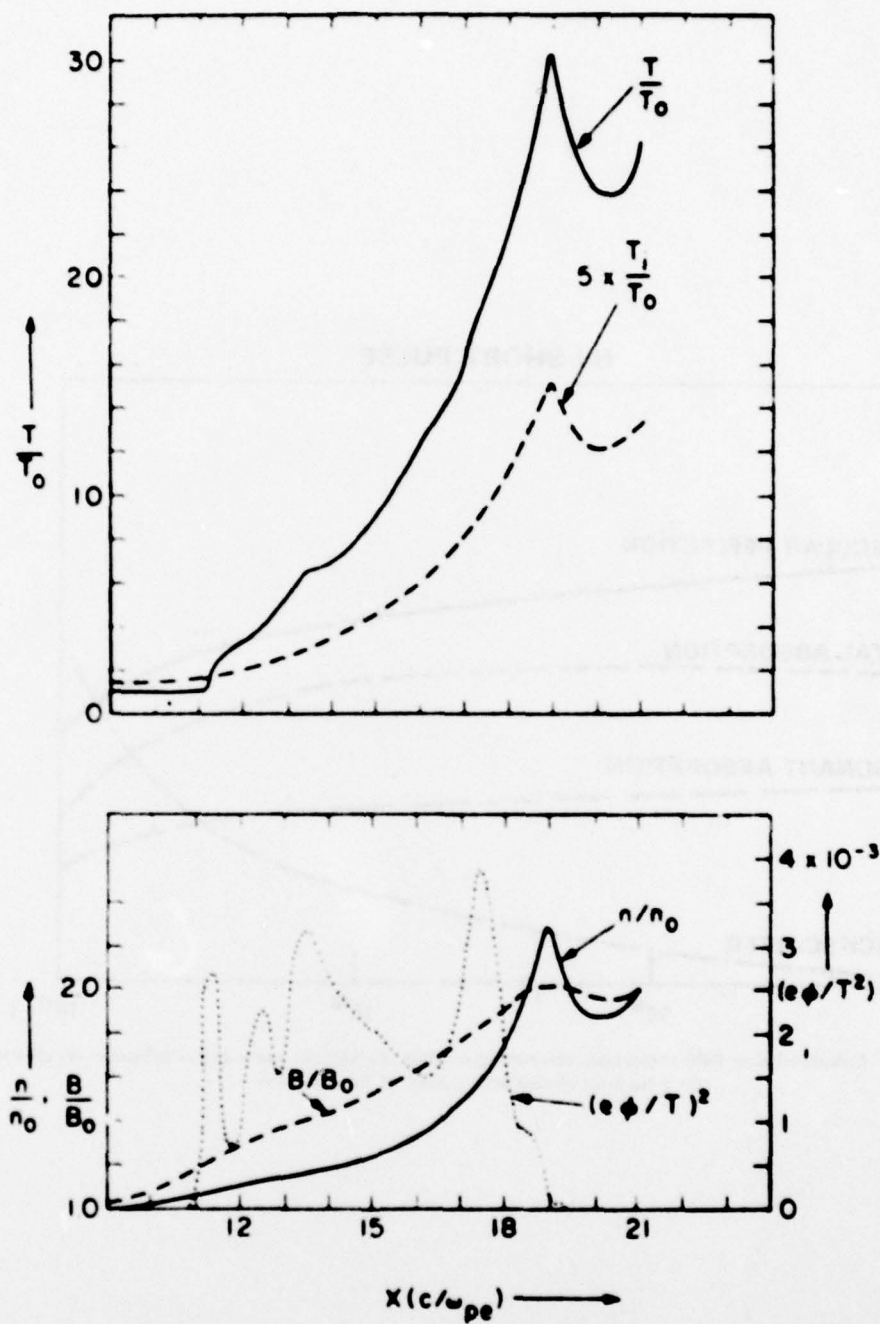


Fig 10 — Plots of density, temperature, magnetic field and turbulence level versus distance for a resistive Mach 2 shock.

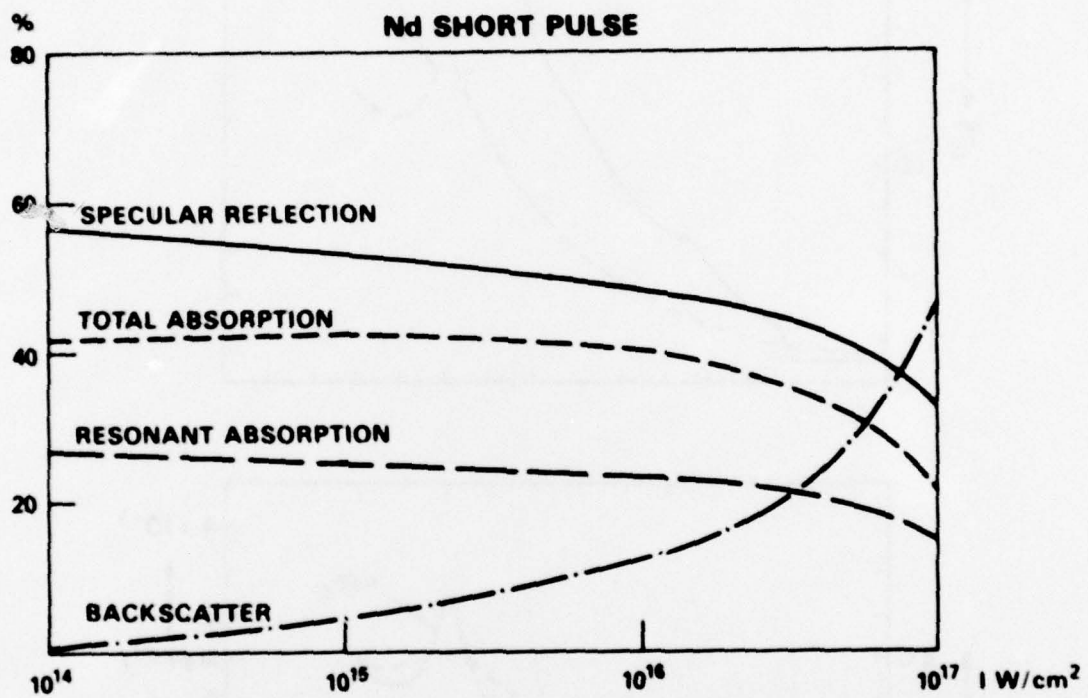


Fig. 11 — Calculated laser light absorption, resonant absorption, backscatter and specular reflection versus irradiance for a Nd laser plasma with a pulse of 70 psec fwhm.

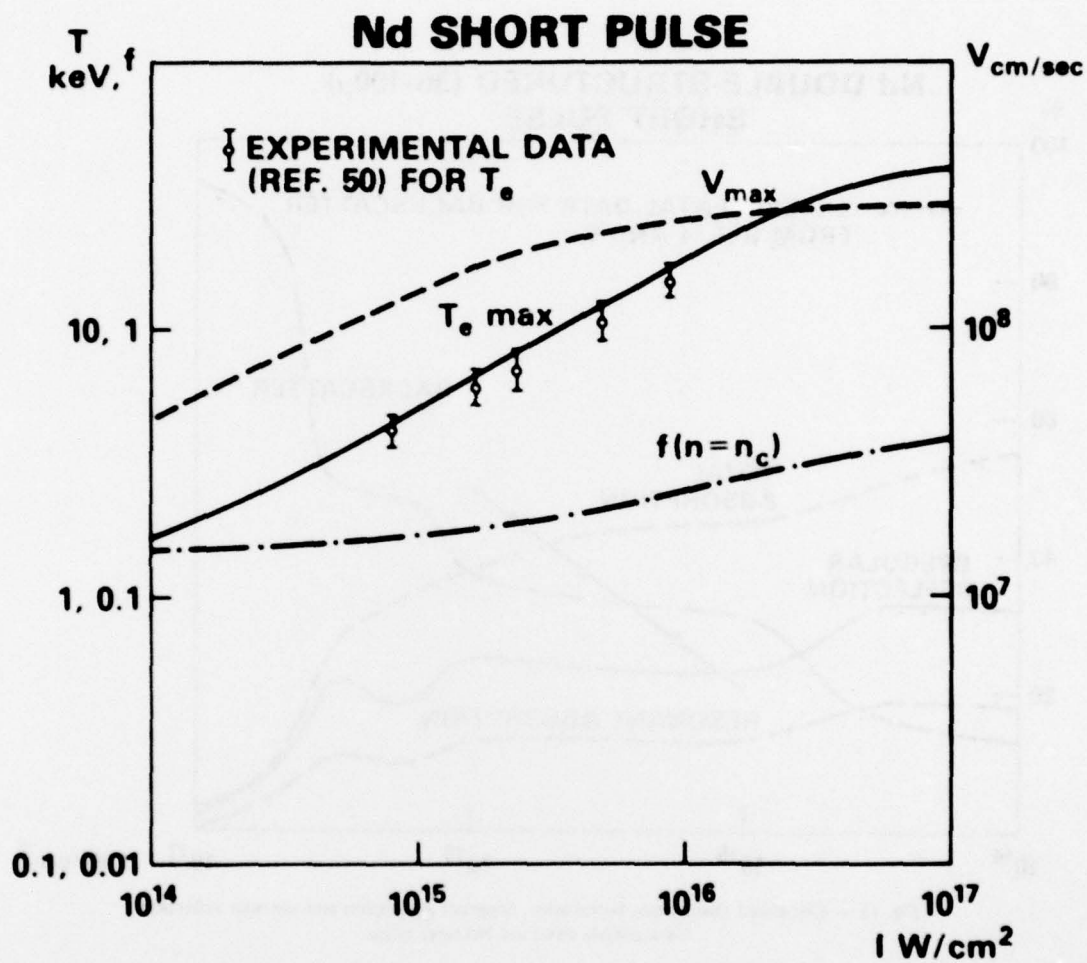


Fig. 12 — Calculations of electron temperature, blowoff velocity and flux limit for the laser pulse of Fig. 11.

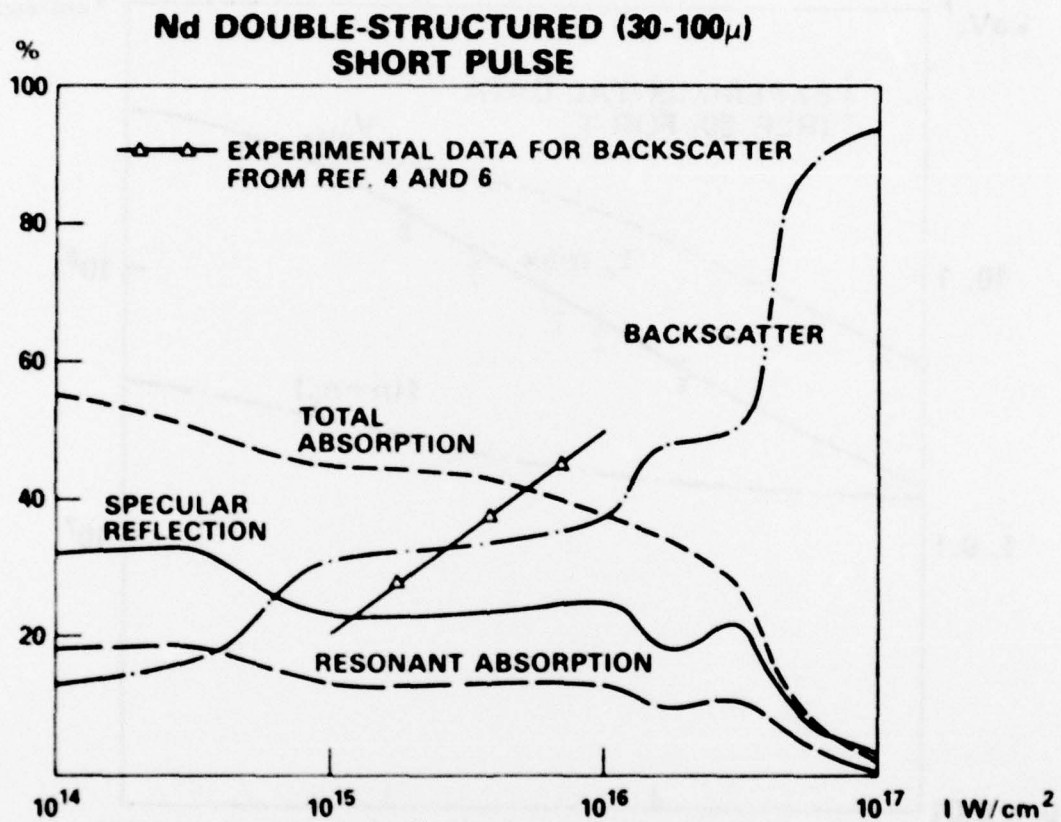


Fig. 13 - Calculated absorption, backscatter, resonant absorption and specular reflection for a double structure Nd laser pulse.

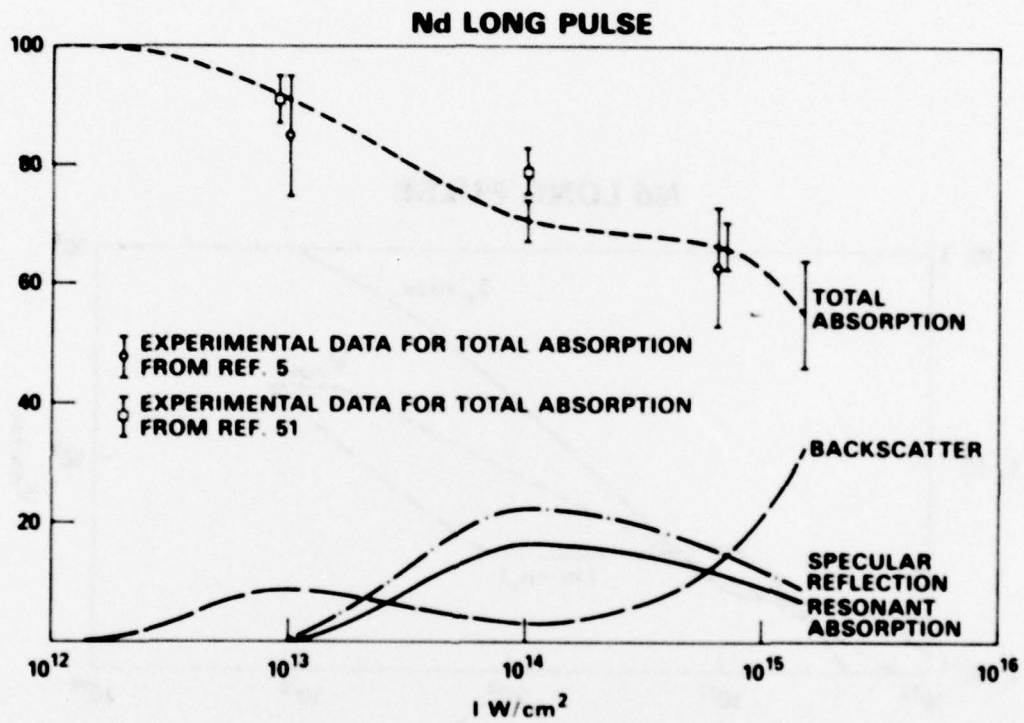


Fig. 14 — As in Fig. 11 for a Nd laser, long pulse.

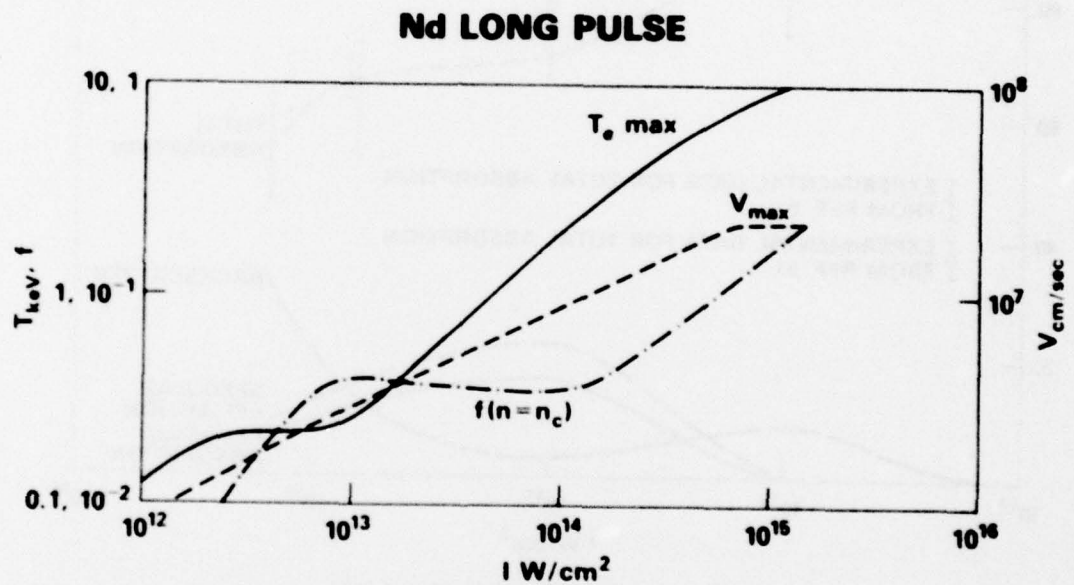


Fig. 15 — As in Fig. 12 for a Nd laser long pulse.